Journal of proteome research

ARTICLE

pubs.acs.org/jpr

# Analysis of Differential Proteomes of Induced Pluripotent Stem Cells by Protein-Based Reprogramming of Fibroblasts

Jonghwa Jin,[†,#] Yoo-Wook Kwon,[§,⊥,#] Jae Seung Paek,[§] Hyun-Jai Cho,[‡,§,∥,⊥] Jiyoung Yu,[†] Ji Yoon Lee,[¶] In-Sun Chu,[⊗] In-Hyun Park,[◆] Young-Bae Park,[‡,§,∥,⊥] Hyo-Soo Kim,[*,‡,§,∥,⊥,○] and Youngsoo Kim[*,†]

Departments of [†]Biomedical Sciences and [‡]Internal Medicine, Seoul National University College of Medicine, Seoul, Korea

[§]National Research Laboratory for Cardiovascular Stem Cell, [∥]Cardiovascular Center and [⊥]Innovative Research Institute for Cell Therapy, Seoul National University Hospital, Seoul National University, Seoul, Korea

[¶]National Instrumentation Center for Environmental Management and [○]Molecular Medicine and Biopharmaceutical Sciences, Seoul National University, Seoul, Korea

[⊗]Korean Bioinformation Center, Korea Research Institute of Bioscience and Biotechnology, 111 Gwahangno, Yuseong-gu, Daejeon 305-806, Korea

[◆]Department of Genetics, Yale University School of Medicine, New Haven, Connecticut 06520, United States

Supporting Information

**ABSTRACT:** The recent generation of induced pluripotent stem (iPS) cells represents a novel opportunity to complement embryonic stem (ES) cell-based approaches. iPS cells can be generated by viral transduction of specific transcription factors, but there is a potential risk of tumorigenicity by random retroviral integration. We have generated novel iPS (sFB-protein-iPS) cells from murine dermal fibroblasts (FVB-sFB) that have ES cell characteristics, using ES cell-derived cell extracts instead of performing viral transduction. Notably, only cell extracts from an ES cell line (C57-mES) on the C57/BL6 background generated iPS cells in our protocol—not an ES cell line (E14-mES) on the 129 background. Hypothesizing that determining the differences in these 2 mES cell lines will provide vital insight into the reprogramming machinery, we performed proteomic and global gene expression analysis by iTRAQ and mRNA microarray, respectively. We observed that pluripotent ES cells and ES cell extract-derived iPS cells had differential proteomes and global gene expression patterns. Notably, reprogramming-competent C57-mES cells highly expressed proteins that regulate protein synthesis and metabolism, compared with reprogramming-incompetent 129-mES cells, suggesting that there is a threshold that protein synthetic machinery must exceed to initiate reprogramming.

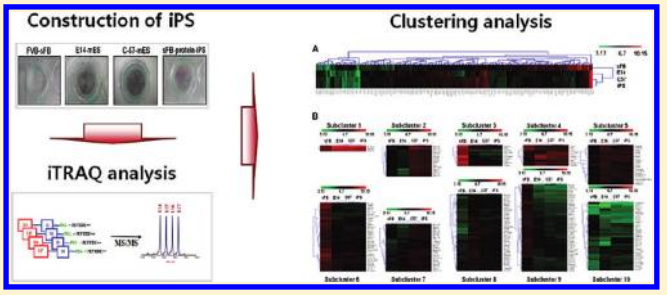


**KEYWORDS:** induced pluripotent stem cell, reprogramming, embryonic stem cell, proteomics, iTRAQ

## INTRODUCTION

Embryonic stem (ES) cells are attractive tools to biological investigators and clinicians due to their pluripotency and self-renewal.[1,2] ES cells have been predicted to be instrumental in screening drug candidates at the development stage and applying cell-based therapies in patients who suffer from degenerative disease and organ failure. Human ES cells have been used to treat Parkinson disease and spinal cord injury.[3]

Yet, many ethical problems exist with regard to human ES cells, because their use implies the destruction of human embryos.[4] Moreover, the application of ES cells is limited to patient- or disease-specific cell-based therapy. These issues can be overcome by generating pluripotent cells from patients' somatic cells, that is, the generation of induced pluripotent stem (iPS) cells might represent the ideal solution for these hurdles.

iPS cells can be generated by viral transduction of specific combinations of transcription factors, such as Oct3/4, Sox2, Nanog, and c-Myc[5] or Oct3/4, Sox2, Nanog, and Lin28.[6] But, this method is associated with potential risks, such as un expected long-term genomic instability and tumorigenicity by random genetic integration due to the use of oncogenic simulators.[7,8] These critical issues must be addressed prior to clinical application.

We have generated ES cell-like pluripotent skin fibroblasts (sFB-protein-iPS) from adult mouse skin fibroblasts using mouse ES (mES) cell-derived soluble proteins.[9] In our protocol, we did not use genetic manipulation or genetic materials to create the iPS cells; instead, we administered mES cell-derived soluble proteins to mouse somatic cells. We also noted that the reprogrammed cells altered their somatic cell properties and became mES-like cells.[9] We did not know, however, which proteins

**Received:** June 19, 2010
**Published:** December 22, 2010

influenced the induction of pluripotent cells and which molecular functions and biological processes governed the reprogramming of somatic cells into iPS cells. Proteomic profiling has not been performed in iPS cells, nor has it been analyzed with regard to molecular and biological levels.

Differential proteomics approaches can be used to examine biological processes by revealing unknown biological functions and cellular signaling pathways.[10,11] In particular, MS/MS spectrometry that is based on Isobaric Tags for Relative and Absolute Quantification (iTRAQ) has been developed, in which reporter ions are differentially and isotopically labeled with isobaric tags that represent the relative concentrations of specific peptides in a mixture of complex proteins.[12]

In a previous study, we obtained iPS cells using extracts from a particular strain of mES cells.[9] Notably, only mES cells from the C57 strain supplied protein that successfully drove the conversion of somatic cells into iPS cells;[9] extracts from 129-background E14-mES cells failed to effect pluripotency. In this regard, we compared the differences in cell extracts between these mES cell lines and noted remarkable disparities between them.

In this report, we used the iTRAQ technique to identify and quantify differential proteomes during the reprogramming of somatic cells into iPS cells. In addition, we examined the mRNA expression during reprogramming of whole transcripts of stem cell-specific transcription factors (Nanog, Oct-4, SOX2, ZFP42, RIF1, UTF1, and ZIC3)[13] and stem cell-specific expressed genes (Catenin α-1, ERAS, DPPA5, ESRRB, FGF4, RNF2, STELLA, and TCL1)[13] by microarray. Consequently, our report might lead to a better understanding of cellular and molecular functions during the reprogramming of somatic cells into iPS cells.

## MATERIALS AND METHODS

### Cell Culture and Reprogramming

C57BL/6-ES cells (C57-mES cells, American Type Culture Cells (ATCC) Catalog No. SCRC-1002), 129-background E14-ES cells (E14-mES cells were generously provided by Jeong Mook Lim, Seoul National University), and reprogrammed skin fibroblast cells were cultured on mitomycin C (Sigma-Aldrich)-treated STO cells in 0.1% gelatin (Sigma-Aldrich)-coated tissue culture dishes. Skin fibroblasts were cultured primarily from the dermis of 8-week-old FVB mice (FVB-sFBs). The protocol for generating reprogrammed cells from FVB-sFBs is described elsewhere.[14,15]

### Western Blot Analysis

To characterize the FVB-sFBs (FVB-background skin fibroblasts), E14-mES (129-background mouse ES cells), C57-mES (C57BL/6-background mouse ES cells), and sFB-protein-iPS (reprogrammed skin fibroblasts) cells, Western blots for Oct-4, Nanog, Eras, and c-Myc were performed. Each sample (30 μg) was separated by 10% SDS-PAGE for 3 h at 50 or 100 V and transferred onto PVDF membranes (GE Healthcare Life Sciences, Buckinghamshire, U.K.) for 1 h at 100 V. PVDF membranes were blocked with 5% (w/v) skim milk in TBS-T (Tris-base 20 mM, 150 mM NaCl, pH 7.4) for 2 h and incubated with antibodies against NANOG (ab80892, 1:1000 dilution, Abcam, Cambridge, U.K.), Oct4 (sc-9081, 1:1000 dilution, Santa Cruz, Inc.), ERAS (sc-51072, 1:1000 dilution, Santa Cruz, Inc.), c-Myc (#2276, 1:1000 dilution, Cell Signaling Technology, Inc.), or β-actin (sc-8432, 1:1000 dilution, Santa Cruz, Inc.) at 4 °C overnight. The secondary antibodies goat anti-mouse IgG-HRP (sc-2031, 1:5000, Santa Cruz, Inc.) and goat anti-rabbit IgG (H+L)-HRP (81-1620, 1:5000, Zymed Laboratories, Inc.) were added for 1 h at room temperature after the membranes were washed.

### Microarray Analysis

Microarray analysis was performed as described.[10] Total RNA from FVB-sFB, E14-mES, C57-mES, and sFB-protein-iPS cells was prepared using the RNeasy Plus Mini Kit 50 (Qiagen, Inc.). RNA quality was verified before microarray analysis. Microarray analyses were performed using mouse whole-genome BeadChips (Illumina, Inc.). Samples were prepared according to the instructions provided by the manufacturer. To detect different probes (differentially expressed genes, DEGs) between C57-mES, E14-mES, FVB-sFB, and sFB-protein-iPS cells, the Benjamin & Hochberg False Discovery Rate (FDR) was measured to enhance the significance in multiple testing. The significance level was set to below an FDR of 5% and a $p$-value of 0.01.

### iTRAQ Labeling and Fractionation by HPLC

iTRAQ labeling and fractionation were performed as described.[10] In brief, FVB-sFB, E14-mES, C57-mES, and sFB-protein-iPS cells were lysed using a modified freeze−thaw lysis method. A total of 100 μg of each protein was reduced, alkylated, digested, and labeled according to the manufacturer's instructions (Applied Biosystems). In this study, FVB-sFB, E14-mES, C57-mES, and sFB-protein-iPS cells were labeled with 114, 115, 116, and 117 reporter ions, respectively. The iTRAQ experiments were performed in duplicate. The labeled iTRAQ samples were separated into 42 fractions by strong cation exchange chromatography (SCX) on an Agilent 1100 (Agilent Technologies) with an SCX column (4.6 mm i.d. × 100 mm, 5 μm, 200 Å, PolyLC, Columbia, MA).

### LC−MS/MS Analysis

LC−MS/MS experiments were performed essentially as described.[10] In brief, we used a hybrid quadrupole-TOF LC−MS/MS spectrometer (Q-Star Elite, Applied Biosystems) that had a nanoelectrospray ionization source and was fitted with a fused silica emitter tip (New Objective, Inc.). For each LC−MS/MS run, 1−2 μg of fractionated peptides was injected into the LC−MS/MS system, and the peptides were trapped and concentrated on an Agilent Zorbax 300SB-C18 column (300 μm i.d. × 50 mm, 5 μm, 100 Å, Agilent Technologies). The peptide mixture was separated on an Agilent Zorbax 300SB nanoflow C18 column (75 μm i.d. × 150 mm, 3.5 μm, 100 Å, Agilent Technologies) at a flow rate of 300 nL/min, and eluted peptides were electrosprayed through a coated silica tip (ion spray voltage at 2300 eV).

### Mass Spectrometric Data Analysis

The data were analyzed essentially as described.[10] In brief, ProteinPilot Software 2.0.1 (Applied Biosystems, Software Revision Number: 67476; Applied Biosystems, User Manual) was used to identify peptides and proteins and quantify differentially expressed proteins. To process an MS or MS/MS spectrum, a thorough search was performed against a human CDS database (human_UnicombinedPANTHER_20061012.fasta, 66 082 entries) using the Paragon and Pro Group algorithms (Applied Biosystems, User Manual).[16] The Unicombined PANTHER database contains 2 databases (Swiss-Prot and TrEMBL), which are combined with PANTHER ontology, allowing each identified protein to be classified and annotated with its "biological process" and "molecular function." Search parameters for this iTRAQ analysis were established similarly as described.[10]

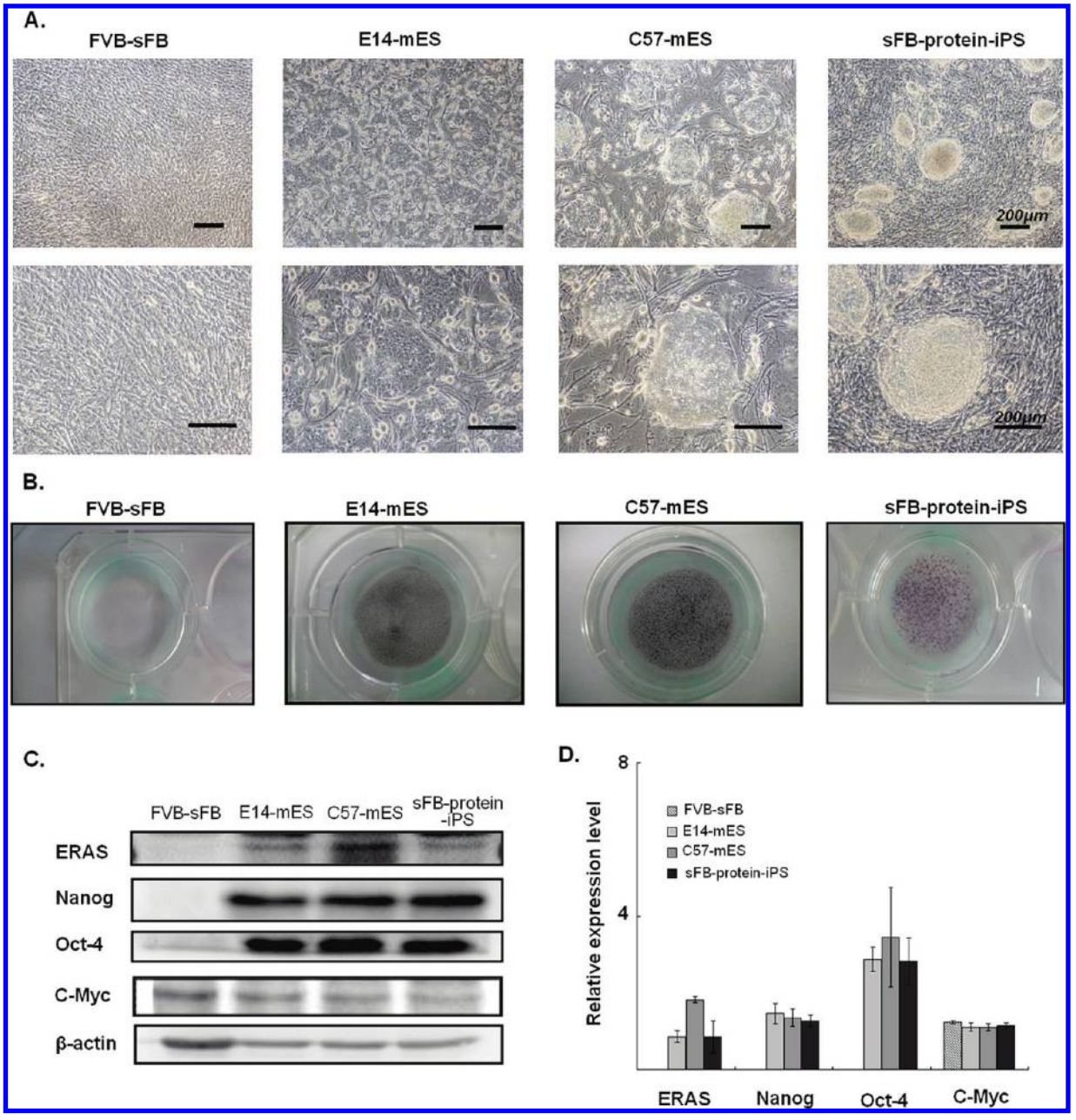


**Figure 1.** Functional characterization of FVB-sFB, mES, and sFB-protein-iPS cells. (A) Somatic cells (skin fibroblasts) were cultured from the dermis of 8-week-old FVB mice. ES cells (E14-mES and C57-mES) from E14 and C57 mouse ES cells were cultured on a mitomycin C-treated STO feeder layer in a 0.1% gelatin-coated tissue culture dish. iPS cells (sFB-protein-iPS) were cultured with passages 5 to 7 (cultured 45−55 days). (B) Alkaline phosphatase (ALP) staining of FVB-sFB, E14-mES, C57-mES, and sFB-protein-iPS cells to assess the level of stemness for each cell. (C) Western blots for ERAS, Oct4, Nanog, and c-Myc in FVB-sFB, mES, and sFB-protein-iPS cells. $\beta$-Actin was used as a loading control. (D) Western blots ($N = 3$) for the four cell types were quantified, with the standard deviations represented by bars.

To validate accurate confidence levels and quantitation values in protein identification and quantitation, the Paragon and Pro Group algorithms used special indications, such as ProtScore, Unused ProtScore, and EF factor. These factors were calculated as follows: ProtScore = −log (1 − percentage confidence/100),[10,16,17] EF = $10^{(95\%\text{-confidence-interval})}$, in which the 95% confidence interval was calculated as (reported ratio × error factor) − (reported ratio/error factor).[10,16,17] Moreover, this software calculates a percentage confidence that reflects the probability that a hit is a false positive; thus, at the 95% confidence level, there is a false positive identification rate of roughly 5%.[16,17] To define significant changes in protein expression, fold-changes >1.25 or <0.8 were established as cutoff values, whereby the cutoff was determined using the experimental replicate method, as described in the Results section.[10,18,19]

## Cluster Analysis

To analyze entire protein profiles more effectively, we performed clustering analysis on differently expressed proteomes using MultiExperiment Viewer (http://www.tm4.org/mev/).[20] MultiExperiment Viewer (Version 4.3) is an application that allows the user to view processed microarray slide representations and identify genes and expression patterns of interest. Slides can

be viewed individually in detail or in groups for comparison. A variety of normalization algorithms and clustering analyses give the user flexibility in creating meaningful views of the expression. For the cluster analysis of differentially expressed proteins, we used the iTRAQ area value for each reporter ion. To calculate the area value for each reporter ion, we first selected the peptides that were used to quantify protein expression of the entire peptide list and then calculated the average values for each peptide.

Hierarchical clustering (HLC) was conducted based on the average area value for differentially expressed proteins. To classify differentially expressed proteins, the distance metric was used to calculate the tree structure, and dendrograms were set by default values, such as Euclidean. To measure the cluster-to-cluster distance, the average distance was used. For more effective clustering of differentially expressed proteins, a support trees module, which offers statistical support for each node of the tree, was used based on resampling of the data. A bootstrapping method was used as a resampling method in the clustering stage.

Furthermore, to examine specific expression patterns, we divided the entire cluster into 10 subclusters based on K-Means/K-Medians Clustering (KMC). The number of clusters $k$ was set to 10. Finally, to analyze the relationship between the clustering results and metabolic and signaling pathways, the DAVID Bioinformatics Resources (http://david.abcc.ncifcrf.gov/) and KEEG databases (http://www.genome.jp/kegg/) were used.

## RESULTS

### Generation of iPS Cells by Transduction of Protein from ES Cells

We have generated reprogrammed skin fibroblast-like pluripotent stem cells (sFB-protein-iPS) from adult skin fibroblasts using proteins from mES cell extracts.[9] Like iPS cells that have been generated by retro- or lentiviral transduction, sFB-protein-iPS cells acquire complete pluripotency, as evidenced by germline transmission by tetraploid complementation. Nevertheless, we could not identify the mES cell proteins that induced the reprogramming of FVB-sFB into sFB-protein-iPS cell or the biological functions that were associated with reprogramming. Thus, we examined their proteomes with regard to reprogramming and classified differentially expressed proteins into functional groups according to differentiated cell type.

To compare proteomic and global gene expression, we used mES cells (C57-mES and E14-mES) from 2 mouse strains (C57/BL6, 129), cell extract-mediated reprogrammed skin fibroblasts (sFB-protein-iPS), and skin fibroblasts (FVB-sFBs). sFB-protein-iPS cells and mES cells had similar morphologies (Figure 1A). sFB-protein-iPS cells showed ES cell-like properties, including the expression of alkaline phosphatase (ALP) (Figure 1B) and stem cell-specific genes (Nanog, Oct4, ERAS) (Figure 1C,D). Global gene expression analysis by microarray confirmed the expression of pluripotency genes in sFB-protein-iPS cells (Supplementary Table S1).

### Analysis of Differential Proteomes by iTRAQ

Our previous analysis of sFB-protein-iPS cells demonstrated that only proteins from mES cell extracts (not RNA) mediated reprogramming.[9] We used iTRAQ to compare protein expression among the FVB-sFB, E14-mES, C57-mES, and sFB-protein-iPS cells.

In this iTRAQ experiment on FVB-sFBs, protein-iPS cells, and mES cells, 1883 proteins were identified from 4029 peptides at a minimum confidence level of 95% (unused ProtScore > 1.3). The detailed protein identification data are shown in Supplementary Table S2. Of the proteins that were identified by iTRAQ, 1% comprised 1-peptide proteins; 1% was 2-peptide proteins; 2% was 3-peptide proteins; 3% was 4-peptide proteins; and 93% was proteins that had 5 or more peptides (Supplementary Figure S1).

### Determination of Cutoff for Significant Fold-Changes in iTRAQ Experiments

In the LC−MS/MS experiments by iTRAQ, labeling efficiency was examined as described, wherein the number of possible labeling sites (lysine side chains and N-termini of all peptides) for iTRAQ tags was compared with that of the detected peptides.[10] The labeling efficiency exceeded 98% for these iTRAQ experiments (data not shown).

To obtain bona fide iTRAQ results, possible variations in the replicate iTRAQ experiments must be identified so as to be minimized.[16,17] In calculating the cutoff threshold for meaningful fold-changes over experimental errors, variations in the experimental replicates were considered to be the actual variations in the 2 iTRAQ experiments, as described.[10] Consequently, in the 2 iTRAQ experiments, 1883 proteins were identified, 727 of which were common. The number of shared quantified proteins in the 2 iTRAQ experiments was 53, based on the following selection criteria: more than 2 unique peptides (>95%) contained, $p$-value < 0.05, and EF < 2 in FVB-sFB, E14-mES, C57-mES, and sFB-protein-iPS cells. These 53 proteins were used initially to determine the experimental variations and to confirm the threshold for meaningful fold-changes.

Experimental variations for the 115/114, 116/114, and 117/114 reporter ions were calculated using the ratios of the 53 common quantified proteins between the first and second iTRAQ experiments, in which the experimental variations were $r^2$=0.9117, $r^2$=0.9241, and $r^2$=0.9116, respectively (Figure 2A). In addition, the cutoff threshold for meaningful fold-changes (defining a so-called "differentially expressed protein") in the expression ratios of 115/114, 116/114, and 117/114 were determined as described.[10] Accordingly, 90% of the identified proteins in the 2 iTRAQ experiments fell within 20% of the respective experimental variation (Figure 2B). Therefore, we stipulated that a fold-change of >1.25 or <0.80 was a meaningful cutoff that represented true differences in the expression of 115/114, 116/114, and 117/114 reporter ions.

In this study, 53 proteins (commonly quantified proteins) were only used to determine cutoff threshold for meaningful fold-changes (so-called differentially expressed proteins), and the number of common differentially expressed proteins ($p$-value < 0.05, EF < 2, more than 2 unique peptides with >95% confidence level, and protein expression > ± 1.25-fold for all reporter ions) was 44 (Supplementary Figure S2).

Although 44 proteins were commonly differentially expressed in the 2 iTRAQ experiments, 225 proteins also met the "differentially expressed proteome rule" (Supplementary Figure S2 and Supplementary Table S3a). Thus, these 225 qualifying proteins from the 2 iTRAQ experiments were selected for further analysis of differential proteomic expression, as follows.

All quantified proteins (225) were classified into "biological process" and "molecular function" categories using human_UnicombinedPANTHER_20061012.fasta, allowing us to analyze phenotypic features and molecular functions in somatic cell reprogramming (Supplementary Table S3a). Selected differentially

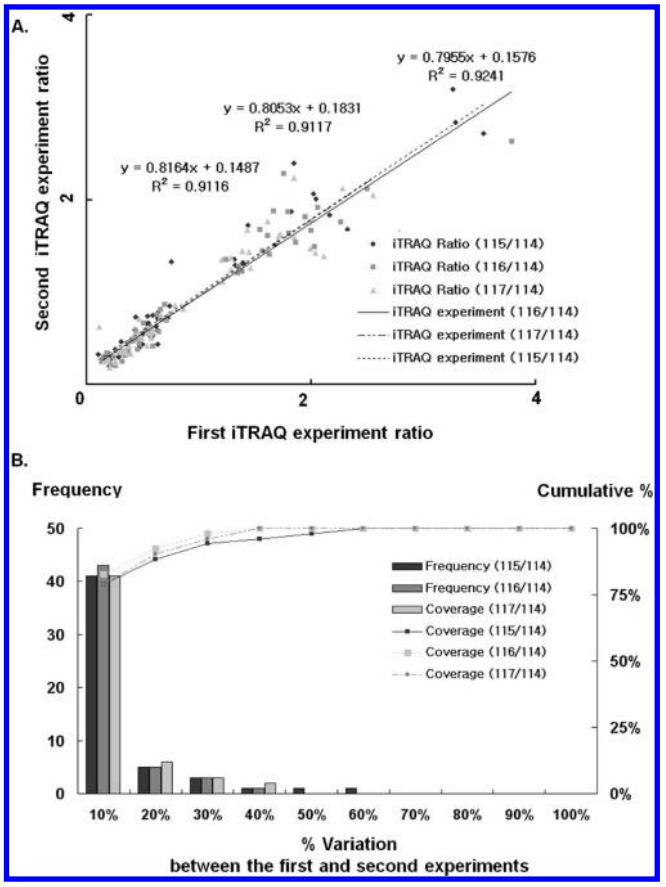


**Figure 2.** Correlation between the two iTRAQ experiments and determination of cutoff value for significant fold-change. (A) Plotting of iTRAQ ratios in E14-mES versus FVB-sFB (115/114), C57-mES versus FVB-sFB (115/114), and sFB-protein-iPS versus FVB-sFB (117/114) cells. The 53 commonly quantitated proteins in the 2 iTRAQ experiments (more than two unique peptides (>95% confidence level), $p$-value < 0.05, and EF < 2) were plotted in the linear dynamic range. The experimental variations yielded a correlation coefficient of $r^2 = 0.9117$, $r^2 = 0.9241$, and $r^2 = 0.9116$ between the first and second iTRAQ experiments, respectively. (B) The % variations between the 2 iTRAQ ratios for the common proteins in the 2 iTRAQ experiments. The 53 quantitated common proteins in the 2 iTRAQ experiments (more than two unique peptides (>95confidence level), $p$-value < 0.05 and EF < 2) were inputted to calculate % variations. The vertical axis represents the number of proteins, and the horizontal axis denotes % variation. The % variation was rounded off to the nearest number. The right vertical axis represents the cumulative % of the counted proteins, in which 100% equals 53 proteins. Ninety percent of the counted proteins fell within a variation of 20%. Therefore, a fold-change >1.25 or <0.80 is a sufficient cutoff that reflects significant changes in the 2 iTRAQ experiments.

expressed proteomes for the "biological process" subcategories are summarized in Supplementary Table S3b. The "molecular function" subcategories accounted for 225 differentially expressed proteins, in which "nucleic acid binding" and "cytoskeleton" represented 23% and 14% of the identified proteins, respectively, the 2 largest components (Supplementary Figure S3).

## Differential Proteomes during Reprogramming of FVB-sFBs into sFB-Protein-iPS Cells

In the comparison of proteome expression in sFB-protein-iPS (117 reporter) versus FVB-sFB cells (114 reporter), all 225 differentially expressed proteins were detected, wherein 124 and 101 were upregulated and downregulated, respectively (Supplementary Figures S4A and S4B and Supplementary Table S3a). In the "biological process" subcategories, the "cell cycle" (81.8% of cells), "cell structure and motility" (88.9%), and "developmental process" (77.8%) subcategories were downregulated during reprogramming of FVB-sFBs into sFB-protein-iPS cells (Figure 3C and Supplementary Tables S3a and S3b). In contrast, 100%, 84.4%, and 79.7% of the 225 proteins were upregulated in the "cell proliferation and differentiation", "nucleotide metabolism", and "protein metabolism" subcategories, respectively (Figure 3C and Supplementary Tables S3a and S3b). The upregulation of "biological process" subcategories is consistent with the functional characterization during reprogramming.

In a comprehensive analysis of protein expression patterns in FVB-sFB, E14-mES, C57-mES, and sFB-protein-iPS cells, we generated scatter plots for the 225 proteins using the area values for each reporter ion (Figure 4A−C and Supplementary Table S3a). As shown in Figure 4A, the protein expression patterns for sFB-protein-iPS versus FVB-sFB cells differed, despite the former having originated from the latter. In contrast, the expression patterns in sFB-protein-iPS and C57-mES cells were similar (Figure 4B), the former of which originated from FVB-sFBs. These differential patterns underlie the conversion of sFB-protein-iPS cells into ES-like cells during reprogramming.

## Comparison of Proteomes between sFB-Protein-iPS versus FVB-sFB Cells and C57-mES versus FVB-sFB Cells

On comparison of the proteomes of C57-mES (116 reporter) versus FVB-sFB (114 reporter) cells, we identified all of the 225 differentially expressed proteins, 124 and 101 of which were upregulated and downregulated, respectively (Supplementary Figures S4A and S4B and Supplementary Table S3a). Notably, these values were the same as those for sFB-protein-iPS (117 reporter) versus FVB-sFB (114 reporter) cells, as described in the previous section.

Further, we observed the same expression patterns in the "biological process" subcategories. Comparing C57-mES versus FVB-sFB cells with sFB-protein-iPS versus FVB-sFB cells, "cell cycle" (81.8%), "cell structure and motility" (88.9%), and "developmental process" (77.8%) were downregulated (Figure 3B and Supplementary Tables S3a and S3b). In contrast, "cell proliferation and differentiation" (100%), "nucleotide metabolism" (84.4%), and "protein metabolism" (79.7%) were upregulated (Figure 3B and Supplementary Tables S3a and S3b). These findings demonstrate that the ES-like status of sFB-protein-iPS cells is similar to C57 m-ES cells. Moreover, by scatter plot, the protein expression patterns of sFB-protein-iPS and C57-mES cells were similar (Figure 4B).

## E14-mES Cell Proteome Differs from That of sFB-Protein-iPS and C57-mES Cells

Between the expression patterns of E14-mES cells (115 reporter) versus FVB-sFB (114 reporter) cells, all 225 differentially expressed proteins were identified, of which 96 and 129 were upregulated and downregulated, respectively (Supplementary Figures S4A and S4B and Supplementary Table S3a). Of the "biological process" subcategories, "cell proliferation and differentiation" (100%), "nucleotide metabolism" (80.6%), and "protein metabolism" (57.8%) were upregulated in E14-mES versus FVB-sFB cells, and "cell cycle" (81.8%), "cell structure and motility" (88.9%), and "developmental process" (77.8%) were downregulated (Figure 3A and Supplementary Tables S3a and S3b). In particular, the expression of proteins in the "nucleotide


dx.doi.org/10.1021/pr100624f |J. Proteome Res. 2011, 10, 977–989

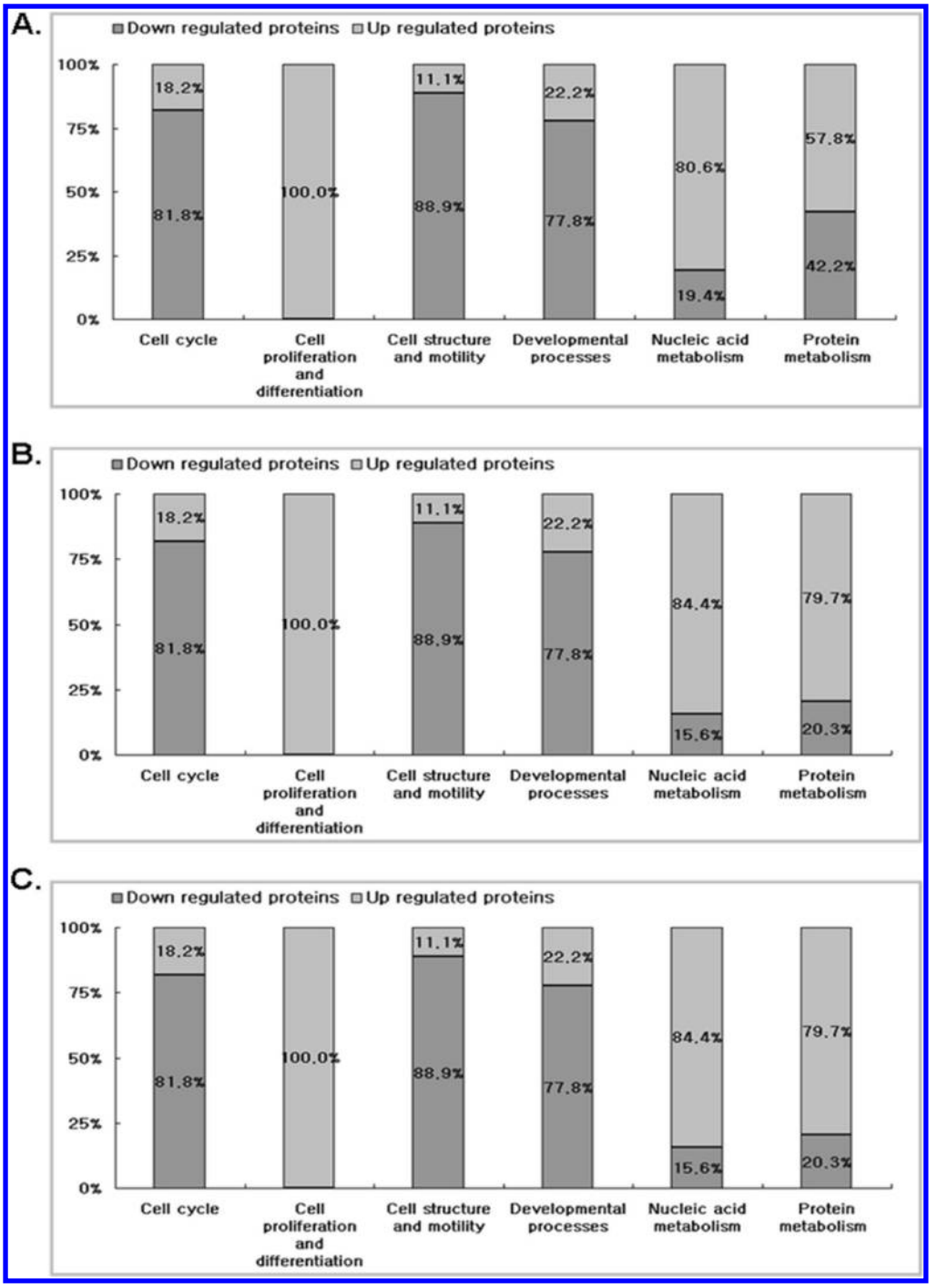


**Figure 3.** Functional classification of differentially expressed proteins in FVB-sFB, mES (E14-mES and C57-mES), and sFB-protein-iPS cells. Functional classification of (A) E14-mES versus FVB-sFB cells, (B) C57-mES versus FVB-sFB cells, (C) sFB-protein-iPS versus FVB-sFB cells. Differentially expressed proteins (225 proteins) in FVB-sFB, mES cells, and sFB-protein-iPS cells were assigned to "biological process" subcategories using human_UnicombinedPANTHER_20061012.fasta, which is interlocked with PANTHER ontology. Only 6 major subcategories for "biological process" are presented, wherein each subcategory is presented as the percentage of up- and downregulated proteins.

metabolism" and "protein metabolism" subcategories changed slightly between C57 mES versus FVB-sFB, sFB-protein-iPS versus FVB-sFB, and E14-mES versus FVB-sFB cells.

Moreover, changes in the expression patterns of the scatter plots were greater in E14-mES versus C57 mES cells compared with sFB-protein-iPS versus C57-mES cells (Figure 4B,C), implying that the biological properties of sFB-protein-iPS cells approximate those of C57 mES cells more closely than to those of E14-mES cells.

## Cluster Analysis of Differentially Expressed Proteomes

The MultiExperiment Viewer (http://mev.tm4.org, Version 4.3)[20] was used to determine the pathways from which differential proteomes were derived during reprogramming. Hierarchical clustering (HLC) was performed on the 225 differentially expressed proteins in FVB-sFB, E14-mES, C57-mES, and sFB-protein-iPS cells by merging or splitting the individual elements, based on one-way clustering methods (Figure 5A).[21]

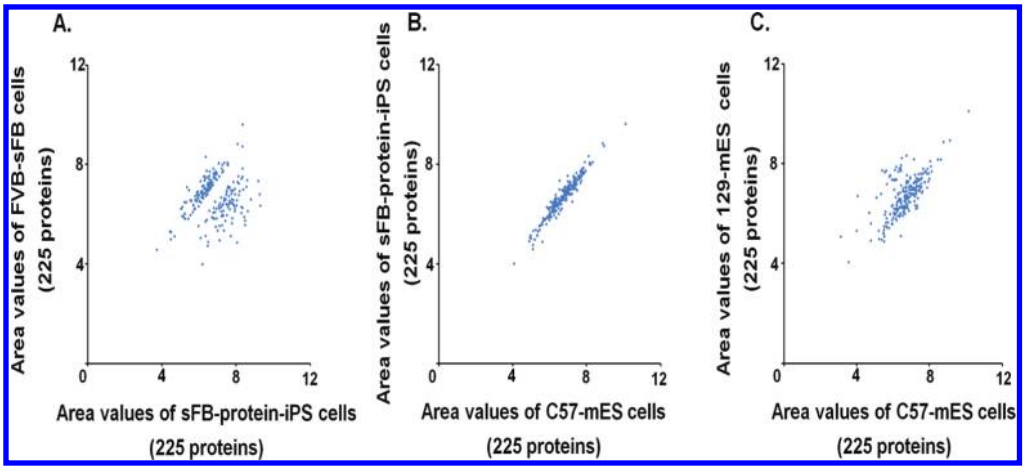


**Figure 4.** Scatter plots for differentially expressed proteins in FVB-sFB, mES, and sFB-protein-iPS cells. Scatter plots for 225 differentially expressed proteins in FVB-sFB, mES, and sFB-protein-iPS cells. Scatter plots as determined by iTRAQ; entire protein expression patterns were compared between (A) FVB-sFB and sFB-protein-iPS cells, (B) sFB-protein-iPS and C57-mES cells, and (C) E14-mES and C57-mES cells. The scatter plots were generated by $\log_2$ transformation of each area value.

Notably, sFB-protein-iPS and C57-mES cells were clustered similarly, whereas E14-mES and FVB-sFB cells were not clustered with C57-mES or sFB-protein-iPS cells. As in the scatter plots, the pattern of hierarchical clustering for sFB-protein-iPS cells was similar to that of C57-mES cells but not to FVB-sFBs (Figure 5A).

Further, we divided the 225 proteins into 10 subclusters by K-Means/K-Medians Clustering (Supplementary Table S3a, Figure 5B); thereafter, the average expression ratios of the proteins were calculated for each subcluster (Figure 5C). Proteins between FVB-sFB and sFB-protein-iPS cells were differentially expressed in all subclusters except 1 and 10, whereas C57-mES and sFB-protein-iPS cells had similar expression patterns in all subclusters (Figure 5B, C). Also, in the hierarchical clustering patterns of subclusters 3, 4, 5, 6, and 9, FVB-sFB differed from those of C57-mES, E14-mES, and sFB-protein-iPS cells, whereas the expression ratios of the proteins in these subclusters were similar between the pluripotent cell types C57-mES, E14-mES, and sFB-protein-iPS (Figure 5C).

Eighty-seven of 114 proteins in subclusters 3, 4, 5, 6, and 9 represented certain functional differences between FVB-sFB cells and the other 3 groups (C57-mES, E14-mES, and sFB-protein-iPS); 27 of these 114 proteins were not fully characterized; thus, they are not included in the classification (the 87 proteins are listed as Group 1 proteins in Supplementary Table S4).

Differences in protein expression between reprogramming-incompetent E14-mES versus reprogramming-competent C57-mES cells were reflected in subclusters 2, 7, and 8 (Figure 5B,C). Specifically, 38 of 75 proteins in these subclusters represented functions that differentiate E14-mES from C57-mES cells; 37 of the 75 were not fully characterized and are not included in the classification (the 38 proteins are listed as Group 2 proteins in Supplementary Table S4). Clearly, the differentially expressed proteins in subclusters 2, 7, and 8 might shed light on the biological features of various ES cell properties between C57-mES and E14-mES cells. Thus, further examination should provide an understanding of the mechanisms by which ES cell extracts drive reprogramming (Figure 5).

## Understanding Related Metabolic and Signaling Pathways Based on Subclustering Data

We performed cluster analysis on 4 sample sets (FVB-sFB, E14-mES, C57-mES, and sFB-protein-iPS cells) to determine the metabolic and signaling pathways that represented the 10 subclusters. The representative proteins from subclusters 3 (10 proteins), 4 (10 proteins), 5 (19 proteins), 6 (33 proteins), and 9 (42 proteins) were grouped preferentially, characterizing the functional differences between FVB-sFBs and the 3 pluripotent stem cells (E14-mES, C57-mES, and sFB-protein-iPS cells) (Supplementary Table S4, Group 1 proteins). Notably, subclusters 3, 4, 5, 6, and 9 were associated with focal adhesion (8 proteins), regulation of actin cytoskeleton (8 proteins), glutathione (3 proteins), adherens junctions (4 proteins), and leukocyte transendothelial migration (4 proteins) (Supplementary Table S6 and Supplementary Figures S5A−E).

Subsequently, we found that representative proteins from subclusters 2 (15 proteins), 7 (23 proteins), and 8 (37 proteins) were also grouped preferentially, representing functional differences between E14-mES cells and C57-mES or sFB-protein-iPS cells (Supplementary Table S4, Group 2 proteins). Subclusters 2, 7, and 8 correlated with the ribosomal protein map (21 proteins) pathway (Supplementary Table S6, Supplementary Figure S6). These results implicate the importance of protein synthesis in cell extract-based reprogramming.

## Comparative Analysis of mRNA and Protein Expression

To examine differentially expressed mRNA transcripts among the FVB-sFB, E14-mES, C57-mES, and sFB-protein-iPS cells, we performed exon array using the Illumina microarray chip (Illumina, Inc.). In 4 replicate arrays for the 4 cell types, 25 697 genes were identified from 47 769 gene-chip, and 8270 genes were quantitated as follows: the significance level was set to below an FDR of 5% and a $p$-value of 0.01.

A systematic analysis of differential proteomes and genomes was performed to identify the associations between protein and transcript expression patterns during reprogramming of FVB-sFBs into sFB-protein-iPS cells. Protein accession numbers were coupled to the gene name via the ExPASy database.

One hundred seventy-two transcripts of the 225 differentially expressed proteins were observed (a match rate of 76.4% to the corresponding differentially expressed proteins), yielding a correlation coefficient of $r = 0.602$ (E14-mES versus FVB-sFB), $r = 0.629$ (C57-mES versus FVB-sFB), and $r = 0.577$ (sFB-protein-iPS versus FVB-sFB), respectively (Figure 6). The detailed

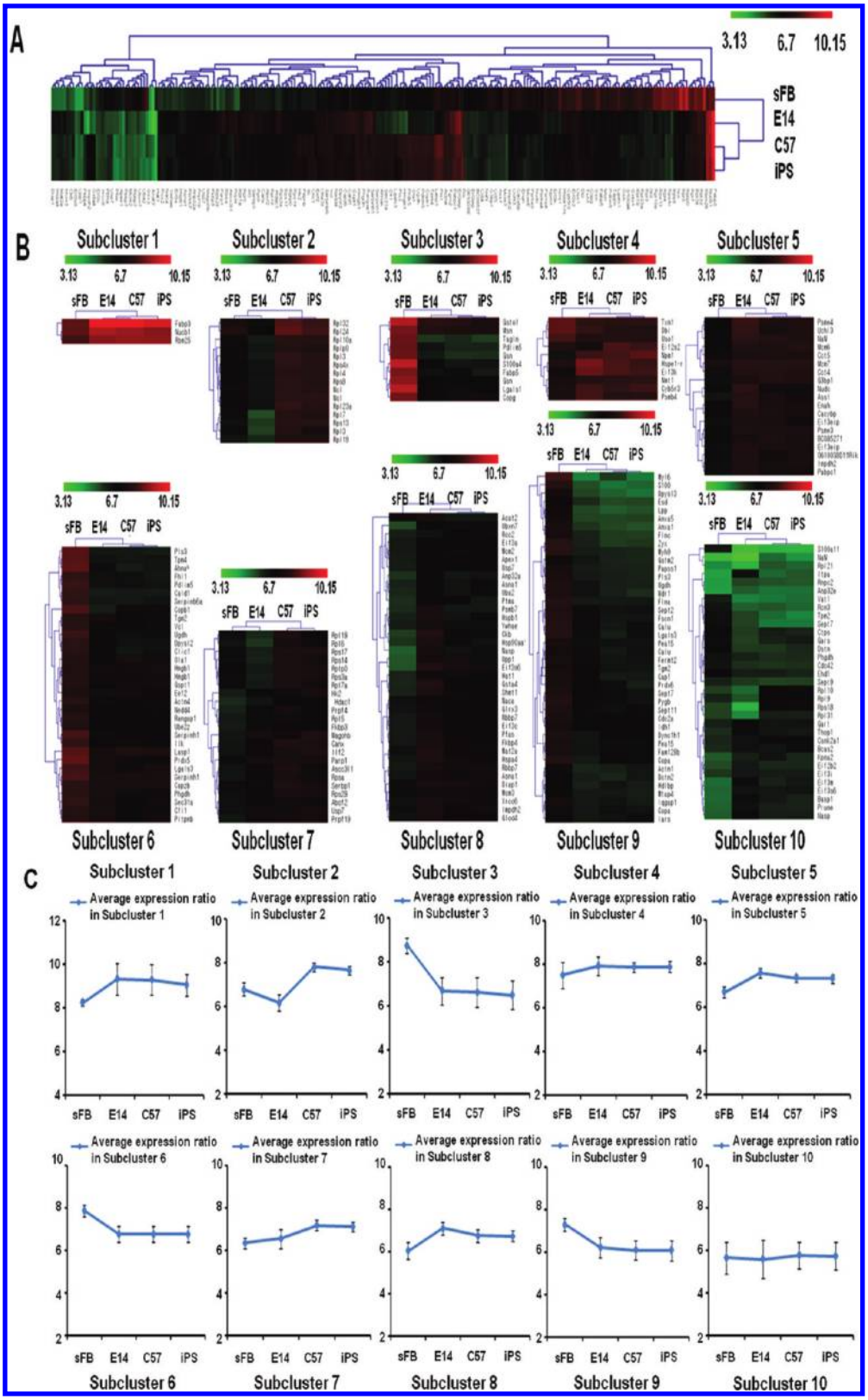


**Figure 5.** Cluster analysis for differentially expressed proteins in FVB-sFB, E14-mES, C57-mES and sFB-protein-iPS cells. Cluster analysis of 225 differentially expressed proteins in FVB-sFB, E14-mES, C57-mES, and sFB-protein-iPS cells. sFB, E14, C57, and iPS represent FVB-sFB, E14-mES, C57-mES, and sFB-protein-iPS cells, respectively. (A) Hierarchical clustering (HLC) was conducted using MultiExperiment Viewer (Version 4.3), based on the average area value for differentially expressed proteins from the iTRAQ experiments. (B) The specific expression patterns were obtained by K-Means/K-Medians Clustering (KMC); the number of clusters *k* was set to 10. (C) Average ratios of the 10 subclusters were calculated for proteins in FVB-sFB, E14-mES, C57-mES, and sFB-protein-iPS cells. sFB, E14, C57, and iPS denote FVB-sFB, E14-mES, C57-mES, and sFB-protein-iPS cells, respectively, and the cluster analysis was performed by $\log_2$ transformation of each area value.


dx.doi.org/10.1021/pr100624f |*J. Proteome Res.* 2011, 10, 977–989

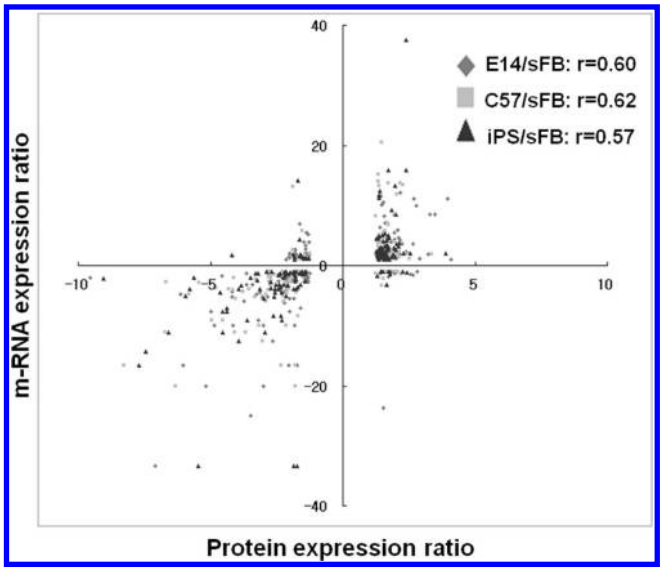


**Figure 6.** Comparison of proteomes and mRNA expression patterns. One hundred seventy-two of the 225 differentially expressed proteins corresponded to their mRNA expression by microarray (a match rate of 76.4% to the differential proteome), generating a correlation coefficient of $r$ = 0.60 (E14-mES versus FVB-sFB, 115/114), $r$ = 0.62 (C57-mES versus sFB, 116/114), and $r$ = 0.57 (iPS versus sFB, 117/114). sFB, E14, C57, and iPS denote FVB-sFB, E14-mES, C57-mES, and sFB-protein-iPS cells, respectively; the cluster analysis was performed by $\log_2$ transformation of each area value.

protein and mRNA expression patterns of the 172 transcripts that were common to the 225 differentially expressed proteins are summarized in Supplementary Table S5.

Furthermore, stem cell-specific genes and transcription factors that regulate stem cell differentiation and development were analyzed. In particular, we found that 15 stem cell markers were preferentially expressed in E14-mES, C57-mES, and sFB-protein-iPS cells versus FVB-sFB (Supplementary Table S1).

## DISCUSSION

### Analysis of Differential Proteomes To Understand Somatic Cell Reprogramming into iPS Cells

Since the generation of iPS cells using retro- or lentiviral vectors that expressed 4 reprogramming factors was reported, attempts have been made to produce clinically safe and usable iPS cells with nonintegrating adenoviruses, transducible recombinant proteins, or chemicals that increase reprogramming efficiency.[22−24] We have successfully generated iPS cells (sFB-protein-iPS) using ES cell extracts.[9] Here, we examined the proteins and processes that regulate the reprogramming of FVB-sFBs.

The chief function of fibroblasts (FVB-sFB cells) is to maintain the structural integrity of connective tissue by secreting extracellular matrix precursors continuously.[25] If FVB-sFB cells are converted into ES-like cells, their fibroblast-like properties should be shed; thus, the expression of proteins that regulate the innate functions of fibroblasts should decline.

In this study, we observed evidence of this conversion. For example, proteins that are related to "cell structure and motility", such as Flnc protein,[26] Filamin-B,[27] Anxa1,[28] Gelsolin,[29] Vinculin,[30] Alpha-actinin-1,[31] Capping protein related,[32] and Alpha-actinin-4,[33] were downregulated during the transformation of FVB-sFBs into sFB-protein-iPS cells (Supplementary Table S3b). Similarly, C57-mES cells also expressed lower levels of these proteins than FVB-sFB cells.

Proteins that are related to "cell cycle", such as Caldesmon 1,[34] Cytoplasmic dynein 1,[35] Septin 2,[36] Septin 7,[37] and Septin 11,[38] were also downregulated, suggesting that they impede the cell cycle to induce the reprogramming of FVB-sFBs into sFB-protein-iPS cells. Experiencing continuous cell proliferation and acquiring the potential to differentiate are essential for inducing ES-equivalent properties in somatic cells. Our proteomic analysis demonstrated increased expression of "cell proliferation and differentiation" proteins (such as Ga17[39] and prothymosin alpha[40]) in pluripotent sFB-protein-iPS and C57-mES versus FVB-sFB cells.

By hierarchical clustering, the protein expression pattern in sFB-protein-iPS cells was similar to that of C57-mES cells but not FVB-sFB cells. Moreover, proteins in subclusters 3, 4, 5, 6, and 9 had disparate expression patterns in FVB-sFB versus the 3 ES-like cell types—sFB-protein-iPS, C57-mES, and E14-mES—between which the patterns were similar (Figure 5B,C). Eighty-seven of the 114 protein in subclusters 3, 4, 5, 6, and 9 were differentially expressed between FVB-sFB versus the other 3 groups (Supplementary Table S4). The differentially expressed proteins in these 5 subclusters reflect functional and biological changes during the generation of iPS cells.

The differential proteomes between sFB-protein-iPS and FVB-sFB cells imply a shift in protein expression during somatic cell reprogramming (FVB-sFB) to pluripotent stem cells (sFB-protein-iPS). The "cell cycle" (81.8%), "cell structure and motility" (88.9%), and "developmental process" (77.8%) subproteomes were downregulated during reprogramming (Figure 3C). Notably, the differences between the C57-mES and FVB-sFB cell proteomes were similar to the subproteomic changes during the conversion of FVB-sFB into sFB-protein-iPS cells (Figure 3B), indicating that iPS cells share ES cell-like cell functions with regard to the "biological process" subcategory. For example, proteins that regulate the cell cycle (Caldesmon 1,[34] Cytoplasmic dynein 1,[35] Septin 2,[36] Septin 7,[37] and Septin 11[38]), cell structure (Flnc protein,[26] Filamin-B,[27] Anxa1,[28] Gelsolin,[29] Vinculin,[30] Alpha-actinin-1,[31] Capping protein,[32] and alpha-Actinin-4[33]), and development (FHL-1,[41] Lipoma-preferred partner homologue,[42] PDZ and LIM domain protein 5,[43] ENH1,[43] Tropomyosin alpha-4,[44] and Tpm2 protein[45]) were downregulated in sFB-protein-iPS versus FVB-sFB cells and C57-mES versus FVB-sFB cells (Supplementary Table S3b).

Moreover, proteins that control "cell proliferation and differentiation" (Ga17 protein,[39] Dendritic cell protein GA17,[39] and prothymosin protein[40]) and "nucleic acid metabolism" (27 proteins) were upregulated in both sFB-protein-iPS versus FVB-sFB cells and C57-mES versus FVB-sFB cells (Supplementary Table S3b). Consequently, the similarity in proteomic differences between sFB-protein-iPS versus FVB-sFB cells and C57-mES versus FVB-sFB cells indicates that sFB-protein-iPS cells attain an ES-equivalent status with regard to protein expression (Figure 3B,C).

Collectively, the differential proteomic data between FVB-sFB versus E14-mES, C57-mES, and sFB-protein-iPS cells and the similarity between sFB-protein-iPS and ES cells (E14 mES, C57-mES) suggest that sFB-protein-iPS cells assume an ES-equivalent state. Thus, a more detailed examination of FVB-sFB reprogramming into sFB-protein-iPS cells might lead to a greater understanding of the mechanism by which iPS cells are generated.


dx.doi.org/10.1021/pr100624f |J. Proteome Res. 2011, 10, 977–989

### Analysis of Differential Proteomes in E14-mES versus sFB-Protein-iPS and C57-mES Cells

sFB-protein-iPS cells were developed using C57-mES cells as the source of protein; protein extracts from E14-mES cell did not generate pluripotent stem cells, spurring us to compare the proteomes between C57-mES and E14-mES cells to examine the differences in components between the 2 caches that mediate the conversion of FVB-sFB into sFB-protein-iPS cells.

We observed differences in expression patterns between C57-mES versus sFB-protein-iPS and E14-mES cells in scatter plots, respectively (Figure 4B,C). The protein expression scatter plots of C57-mES and sFB-protein-iPS cells were similar, unlike those of C57-mES and E14-mES cells, suggesting that C57-mES cells are more similar to sFB-protein-iPS than to E14-mES cells, although C57-mES and E14-mES cells have ES cell properties. Therefore, we propose that extracts from sFB-protein-iPS cells and C57-mES cells catalyze the generation of secondary iPS cells.

Moreover, the proteomic subclusters of C57-mES cells were grouped more similarly with sFB-protein-iPS cells than E14-mES cells by cluster analysis. Proteins from subclusters 2, 7, and 8 were differentially expressed between E14-mES cells versus C57-mES and sFB-protein-iPS cells (Supplementary Table S3a), representing 12, 11, and 15 proteins (Group 2 proteins in Supplementary Table S4) of 15, 23, and 37 proteins, respectively. In particular, the expression ratios of 21 of the 23 proteins in subclusters 2 and 7 (ribosomal proteins) were downregulated in E14-mES/FVB-sFB (115/114) versus C57-mES/FVB-sFB (116/114) and sFB-protein-iPS/FVB-sFB (117/114) cells, respectively (Supplementary Table S4). These results suggest that there is a threshold above which protein synthetic machinery must be expressed to initiate reprogramming. Conversely, the expression ratios for the 15 proteins in subcluster 8 were upregulated in E14-mES/FVB-sFB (115/114) versus C57-mES/FVB-sFB (116/114) and sFB-protein-iPS/FVB-sFB (117/114) cells, respectively (Supplementary Table S4).

Consequently, these differentially expressed proteins, particularly the ribosomal proteins, might be critical in generating pluripotent stem cells from somatic cells.

### Related Metabolic and Signaling Pathways during Reprogramming

To analyze proteomic changes in metabolic and signaling pathways, we performed a cluster analysis of differentially expressed proteins from iTRAQ. Proteins in the first (3, 4, 5, 6, and 9) and second groups of subclusters (2, 7, and 8) were annotated as metabolic and signaling pathways. The first group was associated with focal adhesion (8 proteins), regulation of actin cytoskeleton (8 proteins), glutathione (3 proteins), adherens junctions (4 proteins), and leukocyte transendothelial migration (4 proteins) (Supplementary Table S6 and Supplementary Figure S5A−E). These proteins were downregulated primarily during reprogramming, indicating that actin polymerization, actin stability, and focal complex assembly are inhibited in E14-mES versus FVB-sFB, C57-mES versus FVB-sFB, and sFB-protein-iPS versus FVB-sFB cells. Furthermore, this result might be attributed to differences between ES and somatic cells; the cell cycle in ES cells proceeds more quickly than in differentiated cells due to a shortened G1 phase, and telomerase activity in ES cell is much higher than in somatic cells.[46]

In contrast, proteins in the second group were related to the ribosomal protein map (21 proteins in subclusters 2 and 7) (Supplementary Table S6 and Supplementary Figure S6). The expression ratios for these proteins were downregulated in E14-mES/FVB-sFB (115/114) cells compared with C57-mES/FVB-sFB (116/114) and sFB-protein-iPS/FVB-sFB (117/114) cells: the expression ratio for the ribosomal protein S13 was 0.587 in E14-mES/FVB-sFB (115/114) cells compared with 2.496 and 2.557 in sFB-protein-iPS/FVB-sFB (116/114) and C57-mES/FVB-sFB (117/114) cells, respectively (Supplementary Table S6). Consequently, these 21 ribosomal proteins and the factors that regulate their expression might be critical in generating pluripotent stem cells with C57-mES extracts.

### Analysis of mRNA Expression in the Reprogramming of FVB-sFB to sFB-Protein-iPS Cells

Stem cell-specific transcription factors (NANOG, Oct-4, SOX2, ZFP42, RIF1, UTF1, and ZIC3)[13] and genes (CATENIN α-1, ERAS, DPPA5, ESRRB, FGF4, RNF2, STELLA, and TCL1)[13] were examined by microarray. NANOG, OCT-4, SOX2, ZFP42, RIF1, UTF1, and ZIC3 mRNA was expressed at greater levels in mES and sFB-protein-iPS cells compared with FVB-sFB cells, and ERAS, DPPA5, ESRRB, FGF4, STELLA, and TCL1 were upregulated in mES and sFB-protein-iPS cells versus somatic cells.

In contrast, CATENIN α-1, which regulates the adhesion of stem cells, and RNF2, a polycomb protein, increased slightly in E14-mES, C57-mES, and sFB-protein-iPS versus FVB-sFB cells (Supplementary Table S1). Thus, the increased mRNA levels of stem cell-specific transcription factors and differentially expressed genes in sFB-protein-iPS cells are evidence of the reprogramming of somatic cells into ES-like cells.

### Quantitation of Stem Cell-Specific Markers

Stem cell-specific proteins, such as OCT4, NANOG, SOX2, ESG1, ERAS, and CATENIN α-1, regulate pluripotency and self-renewal in ES cells.[13] In this study, these factors were identified and quantified by iTRAQ and Western blot.

OCT4 and NANOG, which regulate embryonic development and stem cell pluripotency, were not identified in the iTRAQ experiment due to the limits in sensitivity of Q-TOF LC-MS/MS. In contrast, OCT-4 and NANOG were upregulated in E14-mES, C57-mES, and sFB-protein-iPS cells versus FVB-sFB by Western blot. SOX2, a transcription factor that controls early embryogenesis and embryonic stem cell pluripotency by forming a trimeric complex with OCT4, was detected in iTRAQ at a very low confidence level (data not shown). ESG1, which regulates the maintenance of embryonic stem cell pluripotency,[47] was identified and quantified at a $p$-value > 0.05, EF < 2, and more than 2 unique peptides >95% confidence level and was shown to be upregulated in sFB-protein-iPS, C57-mES, and E14-mES versus FVB-sFB cells.

ERAS, which controls the kinase activity of phosphatidylinositol-3-OH and tumor-like growth processes of embryonic stem cells,[48,49] was also identified with a $p$-value > 0.05, EF > 2, and more than 2 unique peptides >95% confidence level, increasing in sFB-protein-iPS and C57-mES cells versus FVB-sFB cells; its expression did not increase between E14-mES and FVB-sFB cells. Notably, ERAS expression differed between C57-mES, sFB-protein-iPS and E14-mES cells, although $p$-value > 0.05 for all comparisons. Previously, we did not generate complete pluripotent stem cells when the E14-mES strain was used as the source of proteins for reprogramming, possibly because differential ERAS expression between E14-mES and C57-mES cells triggers the reprogramming of somatic cells into iPS cells.

## CONCLUSION

In a previous study, we obtained iPS cells using extracts from a particular strain of mES cells. Notably, only mES cells from the

C57 strain supplied protein that successfully drove the conversion of somatic cells (FVB-sFB) into iPS cells (sFB-protein-iPS); extracts from 129-background E14-mES cells failed to effect pluripotency. We noted remarkable disparities between them.

Therefore, in this report, we used the iTRAQ technique to identify (1883 differentially expressed proteins from 4029 unique peptides: *p*-values >95% confidence level, ProtScore >1.3) and quantify differential proteomes (all 225 differentially expressed proteins were detected, wherein 124 and 101 were upregulated and downregulated, respectively) during the reprogramming of somatic cells into iPS cells, including mES cells. Our analysis of differential proteomes using iTRAQ indicated that sFB-protein-iPS cells attain an ES-equivalent status with regard to protein expression, and C57-mES cells are more similar to sFB-protein-iPS than to E14-mES cells, although C57-mES and E14-mES cells have ES cell properties. In addition, we examined the mRNA expression of whole transcripts of stem cell-specific transcription factors and stem cell-specific genes by microarray during reprogramming. Consequently, our report might lead to a better understanding of the cellular and molecular functions during the reprogramming of somatic cells into iPS cells.

## ■ ASSOCIATED CONTENT

### Supporting Information

Supplementary Tables and Supplementary Figures that support the presented data are provided. Supplementary Table S1, differentially expressed transcripts for stem cell-specific genes and transcription factors; Supplementary Table S2, identified proteins from the iTRAQ experiments; Supplementary Table S3a, differentially expressed proteins from the iTRAQ experiments; Supplementary Table S3b, differentially expressed proteomes for "biological process" subcategories; Supplementary Table S4, the first and second groups of proteomes; Supplementary Table S5, differentially expressed transcripts and proteins for whole subclusters; Supplementary Table S6, related metabolic and signaling pathways for the first and second groups of proteomes; Supplementary Figure S1, composition of peptides in the entire identified proteins; Supplementary Figure S2, Venn diagrams of differentially expressed proteomes in two iTRAQ experiments; Supplementary Figure S3, classification of differentially expressed proteins into "molecular function" subcategories; Supplementary Figure S4A,B; Venn diagrams of up- and down-regulated proteomes in E14-mES versus FVB-sFB (115/114), C57-mES versus FVB-sFB (115/114), and sFB-protein-iPS versus FVB-sFB (117/114) cells; Supplementary Figures S5A−E, related metabolic and signaling pathways in the first group (subclusters 3, 4, 5, 6, and 9) of the proteome; Supplementary Figure S6, related metabolic and signaling pathways in the second group (subclusters 2, 7, and 8) of the proteome. This material is available free of charge via the Internet at http://pubs.acs.org.

## ■ AUTHOR INFORMATION

### Corresponding Author

*H.-S.K.: Cardiovascular Center, Seoul National University Hospital 28 Yongon-dong Chongno-gu Seoul 110-744 Korea. Tel, 82-2-2072-2226; fax, 82-2-766-8904; e-mail, hyosoo@snu.ac.kr. Y.K.: Department of Biomedical Sciences, Seoul National University College of Medicine, 28 Yongon-Dong, Chongno-Ku, Seoul 110-799 Korea. Tel, 82-2-740-8073; fax, 82-2-741-0253; e-mail, biolab@snu.ac.kr.

### Author Contributions

#These authors contributed equally to this work.

## ■ ACKNOWLEDGMENT

This work was supported by grants from the Korean Health 21 R&D Project (A062260, 00-PJ3-PG6-GN07-001 and A030003), and by the 21C Frontier Functional Proteomics Project of the Korean Ministry of Science and Technology (grant no. FPR 08-A2-110).

## ■ REFERENCES

(1) Evans, M. J.; Kaufman, M. H. Establishment in culture of pluripotential cells from mouse embryos. *Nature* **1981**, *292* (5819), 154–6.

(2) Martin, G. R. Isolation of a pluripotent cell line from early mouse embryos cultured in medium conditioned by teratocarcinoma stem cells. *Proc. Natl. Acad. Sci. U.S.A.* **1981**, *78* (12), 7634–8.

(3) Thomson, J. A.; Itskovitz-Eldor, J.; Shapiro, S. S.; Waknitz, M. A.; Swiergiel, J. J.; Marshall, V. S.; Jones, J. M. Embryonic stem cell lines derived from human blastocysts. *Science* **1998**, *282* (5391), 1145–7.

(4) Takahashi, K.; Yamanaka, S. Induction of pluripotent stem cells from mouse embryonic and adult fibroblast cultures by defined factors. *Cell* **2006**, *126* (4), 663–76.

(5) Takahashi, K.; Mitsui, K.; Yamanaka, S. Role of ERas in promoting tumour-like properties in mouse embryonic stem cells. *Nature* **2003**, *423* (6939), 541–5.

(6) Okita, K.; Nakagawa, M.; Hyenjong, H.; Ichisaka, T.; Yamanaka, S. Generation of mouse induced pluripotent stem cells without viral vectors. *Science* **2008**, *322* (5903), 949–53.

(7) Okita, K.; Ichisaka, T.; Yamanaka, S. Generation of germline-competent induced pluripotent stem cells. *Nature* **2007**, *448* (7151), 313–7.

(8) Aoi, T.; Yae, K.; Nakagawa, M.; Ichisaka, T.; Okita, K.; Takahashi, K.; Chiba, T.; Yamanaka, S. Generation of pluripotent stem cells from adult mouse liver and stomach cells. *Science* **2008**, *321* (5889), 699–702.

(9) Cho, H. J.; Lee, C. S.; Kwon, Y. W.; Paek, J. S.; Lee, S. H.; Hur, J.; Lee, E. J.; Roh, T. Y.; Chu, I. S.; Leem, S. H.; Kim, Y.; Kang, H. J.; Park, Y. B.; Kim, H. S. Induction of pluripotent stem cells from adult somatic cells by protein-based reprogramming without genetic manipulation. *Blood* **2010**, *116* (3), 386–95.

(10) Jin, J.; Park, J.; Kim, K.; Kang, Y.; Park, S. G.; Kim, J. H.; Park, K. S.; Jun, H.; Kim, Y. Detection of differential proteomes of human beta-cells during islet-like differentiation using iTRAQ labeling. *J. Proteome Res.* **2009**, *8* (3), 1393–403.

(11) Sui, J.; Zhang, J.; Ching, C. B.; Chen, W. N. Comparative proteomic analysis of extracellular proteins reveals secretion of T-kininogen from vascular smooth muscle cells in response to incubation with s-enantiomer of propranolol. *Mol. Pharmaceutics* **2008**, *5* (5), 885–90.

(12) Ross, P. L.; Huang, Y. N.; Marchese, J. N.; Williamson, B.; Parker, K.; Hattan, S.; Khainovski, N.; Pillai, S.; Dey, S.; Daniels, S.; Purkayastha, S.; Juhasz, P.; Martin, S.; Bartlet-Jones, M.; He, F.; Jacobson, A.; Pappin, D. J. Multiplexed protein quantitation in Saccharomyces cerevisiae using amine-reactive isobaric tagging reagents. *Mol. Cell. Proteomics* **2004**, *3* (12), 1154–69.

(13) Graumann, J.; Hubner, N. C.; Kim, J. B.; Ko, K.; Moser, M.; Kumar, C.; Cox, J.; Scholer, H.; Mann, M. Stable isotope labeling by amino acids in cell culture (SILAC) and proteome quantitation of mouse embryonic stem cells to a depth of 5,111 proteins. *Mol. Cell. Proteomics* **2008**, *7* (4), 672–83.

(14) Taranger, C. K.; Noer, A.; Sorensen, A. L.; Hakelien, A. M.; Boquest, A. C.; Collas, P. Induction of dedifferentiation, genomewide transcriptional programming, and epigenetic reprogramming by extracts of carcinoma and embryonic stem cells. *Mol. Biol. Cell* **2005**, *16* (12), 5719–35.

(15) Rajasingh, J.; Lambers, E.; Hamada, H.; Bord, E.; Thorne, T.; Goukassian, I.; Krishnamurthy, P.; Rosen, K. M.; Ahluwalia, D.; Zhu, Y.; Qin, G.; Losordo, D. W.; Kishore, R. Cell-free embryonic stem cell extract-mediated derivation of multipotent stem cells from NIH3T3 fibroblasts for functional and anatomical ischemic tissue repair. *Circ. Res.* **2008**, *102* (11), e107–17.

(16) Shilov, I. V.; Seymour, S. L.; Patel, A. A.; Loboda, A.; Tang, W. H.; Keating, S. P.; Hunter, C. L.; Nuwaysir, L. M.; Schaeffer, D. A. The Paragon Algorithm, a next generation search engine that uses sequence temperature values and feature probabilities to identify peptides from tandem mass spectra. *Mol. Cell. Proteomics* **2007**, *6* (9), 1638–55.

(17) Lu, H.; Yang, Y.; Allister, E. M.; Wijesekara, N.; Wheeler, M. B. The identification of potential factors associated with the development of type 2 diabetes: a quantitative proteomics approach. *Mol. Cell. Proteomics* **2008**, *7* (8), 1434–51.

(18) Gan, C. S.; Chong, P. K.; Pham, T. K.; Wright, P. C. Technical, experimental, and biological variations in isobaric tags for relative and absolute quantitation (iTRAQ). *J. Proteome Res.* **2007**, *6* (2), 821–7.

(19) Glen, A.; Gan, C. S.; Hamdy, F. C.; Eaton, C. L.; Cross, S. S.; Catto, J. W.; Wright, P. C.; Rehman, I. iTRAQ-facilitated proteomic analysis of human prostate cancer cells identifies proteins associated with progression. *J. Proteome Res.* **2008**, *7* (3), 897–907.

(20) Chu, V. T.; Gottardo, R.; Raftery, A. E.; Bumgarner, R. E.; Yeung, K. Y. MeV+R: using MeV as a graphical user interface for Bioconductor applications in microarray analysis. *Genome Biol.* **2008**, *9* (7), R118.

(21) Liu, Y.; Shin, S.; Zeng, X.; Zhan, M.; Gonzalez, R.; Mueller, F. J.; Schwartz, C. M.; Xue, H.; Li, H.; Baker, S. C.; Chudin, E.; Barker, D. L.; McDaniel, T. K.; Oeser, S.; Loring, J. F.; Mattson, M. P.; Rao, M. S. Genome wide profiling of human embryonic stem cells (hESCs), their derivatives and embryonal carcinoma cells to develop base profiles of U.S. Federal government approved hESC lines. *BMC Dev. Biol.* **2006**, *6*, 20.

(22) Woltjen, K.; Michael, I. P.; Mohseni, P.; Desai, R.; Mileikovsky, M.; Hamalainen, R.; Cowling, R.; Wang, W.; Liu, P.; Gertsenstein, M.; Kaji, K.; Sung, H. K.; Nagy, A. piggyBac transposition reprograms fibroblasts to induced pluripotent stem cells. *Nature* **2009**, *458* (7239), 766–70.

(23) Zhou, H.; Wu, S.; Joo, J. Y.; Zhu, S.; Han, D. W.; Lin, T.; Trauger, S.; Bien, G.; Yao, S.; Zhu, Y.; Siuzdak, G.; Scholer, H. R.; Duan, L.; Ding, S. Generation of induced pluripotent stem cells using recombinant proteins. *Cell Stem Cell* **2009**, *4* (5), 381–4.

(24) Huangfu, D.; Maehr, R.; Guo, W.; Eijkelenboom, A.; Snitow, M.; Chen, A. E.; Melton, D. A. Induction of pluripotent stem cells by defined factors is greatly improved by small-molecule compounds. *Nat. Biotechnol.* **2008**, *26* (7), 795–7.

(25) Pfannkuche, K.; Neuss, S.; Pillekamp, F.; Frenzel, L.; Attia, W.; Hannes, T.; Salber, J.; Hoss, M.; Zenke, M.; Fleischmann, B.; Hescheler, J.; Saric, T. Fibroblasts facilitate the engraftment of embryonic stem cell-derived cardiomyocytes on three-dimensional collagen matrices and aggregation in hanging drops. *Stem Cells Dev.* **2010**, *19*, 1589–99.

(26) Dalkilic, I.; Schienda, J.; Thompson, T. G.; Kunkel, L. M. Loss of FilaminC (FLNc) results in severe defects in myogenesis and myotube structure. *Mol. Cell. Biol.* **2006**, *26* (17), 6522–34.

(27) van der Flier, A.; Kuikman, I.; Kramer, D.; Geerts, D.; Kreft, M.; Takafuta, T.; Shapiro, S. S.; Sonnenberg, A. Different splice variants of filamin-B affect myogenesis, subcellular distribution, and determine binding to integrin [beta] subunits. *J. Cell Biol.* **2002**, *156* (2), 361–76.

(28) Weng, X.; Luecke, H.; Song, I. S.; Kang, D. S.; Kim, S. H.; Huber, R. Crystal structure of human annexin I at 2.5 Å resolution. *Protein Sci.* **1993**, *2* (3), 448–58.

(29) Lichtenfels, R.; Dressler, S. P.; Zobawa, M.; Recktenwald, C. V.; Ackermann, A.; Atkins, D.; Kersten, M.; Hesse, A.; Puttkammer, M.; Lottspeich, F.; Seliger, B. Systematic comparative protein expression profiling of clear cell renal cell carcinoma: a pilot study based on the separation of tissue specimens by two-dimensional gel electrophoresis. *Mol. Cell. Proteomics* **2009**, *8* (12), 2827–42.

(30) Coll, J. L.; Ben-Ze'ev, A.; Ezzell, R. M.; Rodriguez Fernandez, J. L.; Baribault, H.; Oshima, R. G.; Adamson, E. D. Targeted disruption of vinculin genes in F9 and embryonic stem cells changes cell morphology, adhesion, and locomotion. *Proc. Natl. Acad. Sci. U.S.A.* **1995**, *92* (20), 9161–5.

(31) Frey, N.; Richardson, J. A.; Olson, E. N. Calsarcins, a novel family of sarcomeric calcineurin-binding proteins. *Proc. Natl. Acad. Sci. U.S.A.* **2000**, *97* (26), 14632–7.

(32) Chen, N.; Qu, X.; Wu, Y.; Huang, S. Regulation of actin dynamics in pollen tubes: control of actin polymer level. *J. Integr. Plant Biol.* **2009**, *51* (8), 740–50.

(33) Goto, H.; Wakui, H.; Komatsuda, A.; Ohtani, H.; Imai, H.; Sawada, K.; Kobayashi, R. Renal alpha-actinin-4: purification and puromycin aminonucleoside-binding property. *Nephron Exp. Nephrol.* **2003**, *93* (1), e27–35.

(34) Kohler, C. N. The actin-binding protein caldesmon is in spleen and lymph nodes predominately expressed by smooth muscle cells, reticular cells, and follicular dendritic cells. *J. Histochem. Cytochem.* **2010**, *58*, 183–93.

(35) Rashid, S.; Breckle, R.; Hupe, M.; Geisler, S.; Doerwald, N.; Neesen, J. The murine Dnali1 gene encodes a flagellar protein that interacts with the cytoplasmic dynein heavy chain 1. *Mol. Reprod. Dev.* **2006**, *73* (6), 784–94.

(36) Kinoshita, M.; Kumar, S.; Mizoguchi, A.; Ide, C.; Kinoshita, A.; Haraguchi, T.; Hiraoka, Y.; Noda, M. Nedd5, a mammalian septin, is a novel cytoskeletal component interacting with actin-based structures. *Genes Dev.* **1997**, *11* (12), 1535–47.

(37) Jia, Z. F.; Huang, Q.; Kang, C. S.; Yang, W. D.; Wang, G. X.; Yu, S. Z.; Jiang, H.; Pu, P. Y. Overexpression of septin 7 suppresses glioma cell growth. *J. Neurooncol.* **2010**, *98*, 329–40.

(38) Mostowy, S.; Danckaert, A.; Tham, T. N.; Machu, C.; Guadagnini, S.; Pizarro-Cerda, J.; Cossart, P. Septin 11 restricts InlB-mediated invasion by Listeria. *J. Biol. Chem.* **2009**, *284* (17), 11613–21.

(39) Zhou, C.; Arslan, F.; Wee, S.; Krishnan, S.; Ivanov, A. R.; Oliva, A.; Leatherwood, J.; Wolf, D. A. PCI proteins eIF3e and eIF3m define distinct translation initiation factor 3 complexes. *BMC Biol.* **2005**, *3*, 14.

(40) Carninci, P.; Kasukawa, T.; Katayama, S.; Gough, J.; Frith, M. C.; Maeda, N.; Oyama, R.; Ravasi, T.; Lenhard, B.; Wells, C.; Kodzius, R.; Shimokawa, K.; Bajic, V. B.; Brenner, S. E.; Batalov, S.; Forrest, A. R.; Zavolan, M.; Davis, M. J.; Wilming, L. G.; Aidinis, V.; Allen, J. E.; Ambesi-Impiombato, A.; Apweiler, R.; Aturaliya, R. N.; Bailey, T. L.; Bansal, M.; Baxter, L.; Beisel, K. W.; Bersano, T.; Bono, H.; Chalk, A. M.; Chiu, K. P.; Choudhary, V.; Christoffels, A.; Clutterbuck, D. R.; Crowe, M. L.; Dalla, E.; Dalrymple, B. P.; de Bono, B.; Della Gatta, G.; di Bernardo, D.; Down, T.; Engstrom, P.; Fagiolini, M.; Faulkner, G.; Fletcher, C. F.; Fukushima, T.; Furuno, M.; Futaki, S.; Gariboldi, M.; Georgii-Hemming, P.; Gingeras, T. R.; Gojobori, T.; Green, R. E.; Gustincich, S.; Harbers, M.; Hayashi, Y.; Hensch, T. K.; Hirokawa, N.; Hill, D.; Huminiecki, L.; Iacono, M.; Ikeo, K.; Iwama, A.; Ishikawa, T.; Jakt, M.; Kanapin, A.; Katoh, M.; Kawasawa, Y.; Kelso, J.; Kitamura, H.; Kitano, H.; Kollias, G.; Krishnan, S. P.; Kruger, A.; Kummerfeld, S. K.; Kurochkin, I. V.; Lareau, L. F.; Lazarevic, D.; Lipovich, L.; Liu, J.; Liuni, S.; McWilliam, S.; Madan Babu, M.; Madera, M.; Marchionni, L.; Matsuda, H.; Matsuzawa, S.; Miki, H.; Mignone, F.; Miyake, S.; Morris, K.; Mottagui-Tabar, S.; Mulder, N.; Nakano, N.; Nakauchi, H.; Ng, P.; Nilsson, R.; Nishiguchi, S.; Nishikawa, S.; Nori, F.; Ohara, O.; Okazaki, Y.; Orlando, V.; Pang, K. C.; Pavan, W. J.; Pavesi, G.; Pesole, G.; Petrovsky, N.; Piazza, S.; Reed, J.; Reid, J. F.; Ring, B. Z.; Ringwald, M.; Rost, B.; Ruan, Y.; Salzberg, S. L.; Sandelin, A.; Schneider, C.; Schonbach, C.; Sekiguchi, K.; Semple, C. A.; Seno, S.; Sessa, L.; Sheng, Y.; Shibata, Y.; Shimada, H.; Shimada, K.; Silva, D.; Sinclair, B.; Sperling, S.; Stupka, E.; Sugiura, K.; Sultana, R.; Takenaka, Y.; Taki, K.; Tammoja, K.; Tan, S. L.; Tang, S.; Taylor, M. S.; Tegner, J.; Teichmann, S. A.; Ueda, H. R.; van Nimwegen, E.; Verardo, R.; Wei, C. L.; Yagi, K.; Yamanishi, H.; Zabarovsky, E.; Zhu, S.; Zimmer, A.; Hide, W.; Bult, C.; Grimmond, S. M.; Teasdale, R. D.; Liu, E. T.; Brusic, V.; Quackenbush, J.; Wahlestedt, C.; Mattick, J. S.; Hume, D. A.; Kai, C.; Sasaki, D.; Tomaru, Y.; Fukuda, S.; Kanamori-Katayama, M.; Suzuki, M.; Aoki, J.; Arakawa,

T.; Iida, J.; Imamura, K.; Itoh, M.; Kato, T.; Kawaji, H.; Kawagashira, N.; Kawashima, T.; Kojima, M.; Kondo, S.; Konno, H.; Nakano, K.; Ninomiya, N.; Nishio, T.; Okada, M.; Plessy, C.; Shibata, K.; Shiraki, T.; Suzuki, S.; Tagami, M.; Waki, K.; Watahiki, A.; Okamura-Oho, Y.; Suzuki, H.; Kawai, J.; Hayashizaki, Y. The transcriptional landscape of the mammalian genome. *Science* **2005**, *309* (5740), 1559–63.

(41) Fimia, G. M.; De Cesare, D.; Sassone-Corsi, P. A family of LIM-only transcriptional coactivators: tissue-specific expression and selective activation of CREB and CREM. *Mol. Cell. Biol.* **2000**, *20* (22), 8613–22.

(42) Jin, L.; Yoshida, T.; Ho, R.; Owens, G. K.; Somlyo, A. V. The actin-associated protein Palladin is required for development of normal contractile properties of smooth muscle cells derived from embryoid bodies. *J. Biol. Chem.* **2009**, *284* (4), 2121–30.

(43) Passier, R.; Richardson, J. A.; Olson, E. N. Oracle, a novel PDZ-LIM domain protein expressed in heart and skeletal muscle. *Mech. Dev.* **2000**, *92* (2), 277–84.

(44) Hardy, S.; Fiszman, M. Y.; Osborne, H. B.; Thiebaud, P. Characterization of muscle and non muscle Xenopus laevis tropomyosin mRNAs transcribed from the same gene. Developmental and tissue-specific expression. *Eur. J. Biochem.* **1991**, *202* (2), 431–40.

(45) MacGowan, G. A.; Du, C.; Wieczorek, D. F.; Koretsky, A. P. Compensatory changes in Ca(2+) and myocardial O(2) consumption in beta-tropomyosin transgenic hearts. *Am. J. Physiol.: Heart Circ. Physiol.* **2001**, *281* (6), H2539–48.

(46) Zhao, R.; Daley, G. Q. From fibroblasts to iPS cells: induced pluripotency by defined factors. *J. Cell. Biochem.* **2008**, *105* (4), 949–55.

(47) Western, P.; Maldonado-Saldivia, J.; van den Bergen, J.; Hajkova, P.; Saitou, M.; Barton, S.; Surani, M. A. Analysis of Esg1 expression in pluripotent cells and the germline reveals similarities with Oct4 and Sox2 and differences between human pluripotent cell lines. *Stem Cells* **2005**, *23* (10), 1436–42.

(48) Sorrentino, E.; Nazzicone, V.; Farini, D.; Campagnolo, L.; De Felici, M. Comparative transcript profiles of cell cycle-related genes in mouse primordial germ cells, embryonic stem cells and embryonic germ cells. *Gene Expression Patterns* **2007**, *7* (6), 714–21.

(49) Kaizaki, R.; Yashiro, M.; Shinto, O.; Yasuda, K.; Matsuzaki, T.; Sawada, T.; Hirakawa, K. Expression of ERas oncogene in gastric carcinoma. *Anticancer Res.* **2009**, *29* (6), 2189–93.